bioRxiv preprint doi: https://doi.org/10.1101/2020.02.14.949941; this version posted February 15, 2020. The copyright holder for this preprint (which was not certified by peer review) is the author/funder, who has granted bioRxiv a license to display the preprint in perpetuity. It is made available under aCC-BY-NC 4.0 International license.

Integrin Affinity Modulation Critically Regulates Atherogenic Endothelial Activation *in vitro* and *in vivo*

Zaki Al-Yafeai[1], Jonette M. Peretik[3], Brenna H. Pearson[1], Umesh Bhattarai[1], Dongdong Wang[3], Brian G. Petrich[4], and A. Wayne Orr[1, 2, 3, 5]

Departments of Molecular and Cellular Physiology[1], Cell Biology and Anatomy[2], and Pathology and Translational Pathobiology[3], LSU Health Sciences Center, Shreveport, LA, Department of Pediatrics[4], Emory University, Atlanta, GA.

[5] Corresponding author:
A. Wayne Orr
Department of Pathology and Translational Pathobiology
1501 Kings Hwy
Biomedical Research Institute, Rm. 6-21
LSU Health Sciences Center – Shreveport
Shreveport, LA 71130
Office: (318) 675-5462
Fax: (318) 675-8144
aorr@lsuhsc.edu

Running title: Integrin activation in endothelial inflammation

bioRxiv preprint doi: https://doi.org/10.1101/2020.02.14.949941; this version posted February 15, 2020. The copyright holder for this preprint (which was not certified by peer review) is the author/funder, who has granted bioRxiv a license to display the preprint in perpetuity. It is made available under aCC-BY-NC 4.0 International license.

Abstract

While vital to platelet and leukocyte adhesion, integrin activation's role in adherent cells remains controversial. In endothelial cells, atheroprone hemodynamics and oxidized lipoproteins promote endothelial integrin activation *in vitro*, and integrin inhibitors reduce endothelial activation to these stimuli *in vitro* and *in vivo*. However, integrin activation's importance to endothelial phenotype remains unknown. We now show that integrin activation-deficient endothelial cells (talin1 L325R) adhere and spread, suggesting that integrin activation is dispensable for endothelial cell adhesion. However, talin1 L325R endothelial cells fail to support integrin activation, fibronectin deposition, and proinflammatory responses to atheroprone hemodynamics and oxidized lipoproteins. Rescuing integrin activation in talin1 L325R cells partially restores fibronectin deposition, whereas NF-κB activation and maximal fibronectin deposition require both integrin activation and other integrin-independent signaling. Similarly, atheroprone hemodynamics fail to promote inflammation and macrophage recruitment in endothelial-specific talin1 L325R mice. These studies demonstrate a vital role for integrin activation in regulating endothelial phenotype.

bioRxiv preprint doi: https://doi.org/10.1101/2020.02.14.949941; this version posted February 15, 2020. The copyright holder for this preprint (which was not certified by peer review) is the author/funder, who has granted bioRxiv a license to display the preprint in perpetuity. It is made available under aCC-BY-NC 4.0 International license.

Introduction

In the arterial microenvironment at atherosclerosis prone regions, local hemodynamics and matrix composition critically regulate endothelial activation and early atherosclerosis[1,2]. Disturbed flow primes endothelium to activation by systemic factors, in part through NF- κB activation[3,4]. However, disturbed flow-induced endothelial activation is significantly enhanced in the presence of a fibronectin-rich matrix, whereas endothelial activation is reduced on basement membrane proteins (collagen IV, laminin)[5-7]. Additionally, matrix content plays a vital role in oxidized LDL (oxLDL)-mediated proinflammatory responses, where a fibronectin-rich matrix enhances endothelial activation in response to oxLDL[8,9]. Integrins, the largest family of receptors for extracellular matrix (ECM) proteins, are heterodimers of α and β subunits that mediate both cell-dependent extracellular matrix remodeling and matrix-dependent changes in cell phenotype[10]. Blocking fibronectin-binding integrins suppresses endothelial activation by oxLDL and by disturbed flow both *in vitro* and *in vivo*[8,9,11,12], indicating an important role for these integrin in this context. Therefore, cell-matrix interactions serve as an essential component of early atherogenic endothelial activation.

Endothelial integrins mediate distinct responses based on integrin-ligand pair involved[13]. The fibronectin-binding integrin α5β1 plays a clear role in atherogenic endothelial activation. Atheroprone areas show elevated α5 mRNA and protein expression[14,15], and both disturbed flow and oxLDL induce $\alpha5\beta1$-dependent fibronectin matrix assembly and endothelial proinflammatory responses including NF-κB activation and ICAM-1/VCAM-1 expression[8,9,16]. Showing selective deletion of α5 integrins in the endothelium reduces atherogenic inflammation, and mice expressing an α5/α2 integrin chimera similarly reduces early atherosclerotic plaque formation and atherogenic inflammation, indicating an important role for $\alpha5\beta1$ integrin signaling in early atherosclerosis[16]. Both oxLDL and flow induce $\alpha5\beta1$ integrin activation, a cell-dependent process that converts integrins from a low affinity, bent conformation to a high affinity, extended conformation[17]. Although multiple signaling pathways are implicated in integrin activation, the common final step in modulating integrin activity involves interactions between the cytoplasmic tail of integrin β subunits and the protein talin1[18], a large cytoskeleton protein consisting of a head domain that interacts with the integrin and a rod domain that binds components of the actin cytoskeleton[17]. Upon recruitment to the plasma membrane, the talin1 head domain binds to an NPxY motif on the β integrin subunit which promotes a second interaction between talin1 and the membrane-proximal region (MPR) of the integrin[19].

While well characterized in hematopoietic cells, the role talin1-dependent integrin activation in endothelial cell function remains poorly defined. Global knockout of talin1 is embryonic lethal at 8.5-9.5 days and associated with vascular defects[20]. Inducible talin1 deletion in endothelial cells results in an unstable intestinal vasculature resulting, in hemorrhage and premature death[21]. However, these effects may be due to talin1's role in maintaining cell adhesion rather than integrin activation. A mutation in the talin1 head domain that selectively impairs the ability of talin1 to bind integrin β subunit MPR (L325R)[22,23] prevents integrin activation without affecting talin1's ability to bind the β-integrin subunit and form focal adhesions. Mice expressing only this L325R talin1 mutant in platelets and neutrophils show defects in thrombus formation and neutrophil homing to sites of inflammation, respectively[21,22]. Therefore, we sought to utilize this model to characterize the importance of talin1-dependent integrin activation in endothelial phenotype in the context of atherogenic endothelial activation.

bioRxiv preprint doi: https://doi.org/10.1101/2020.02.14.949941; this version posted February 15, 2020. The copyright holder for this preprint (which was not certified by peer review) is the author/funder, who has granted bioRxiv a license to display the preprint in perpetuity. It is made available under aCC-BY-NC 4.0 International license.

Materials and Methods

Cell culture- Mouse lung endothelial cells were isolated from Talin1$^{fl/L325R}$ mice (gift of Brian Petrich, Emory, Atlanta, GA) as previously described[21]). Briefly, lung tissue was harvested, minced, and pushed through a 16G needle and subjected to enzymatic digestion to obtain a single cell suspension. After sorting with magnetic beads coupled to ICAM2 antibodies (eBiosource), cells were transformed using a retrovirus expressing temperature-sensitive large T-antigen. The floxed allele of talin1 was deleted using adenovirus harboring either GFP (green fluorescence protein)-Cre or GFP alone and then sorted for GFP positivity. Lung endothelial cells were grown in DMEM with 10% fetal bovine serum, 1% penicillin/streptomycin, and 1% glutamax. For endothelial shear stress treatments, cells were plated on 38 x 75 mm glass slides (Corning) at confluency, and slides were assembled into a parallel plate flow chamber as previously described[24]. For acute shear stress, cells were exposed to 12 dynes/cm2 flow for up to 1 hour. For chronic oscillatory flow (model of disturbed flow), cells were exposed to ±5 dynes/cm2 with 1 dyne/cm2 forward flow for media exchange. Human LDL (Intracell) was oxidized by dialysis in PBS containing 13.8 μM Cu2SO4 followed by 50 μM EDTA as previously described[25]. Computationally designed transmembrane α-helical peptides (CHAMP) peptides were a gift of Dr. William DeGrado (University of California – San Francisco)[26].

Western blot- Cell lysis and western blot was done as previously described[25]. Briefly, cells were lysed in 2X laemmli buffer, separated by SDS-PAGE gels and then transferred to polyvinylidene difluoride (PVDF) membranes (Bio-Rad, Hercules, CA). Consequently, membranes were blocked in 5% dry milk in TBST for an hour, then incubated with primary antibodies overnight. Antibodies used include rabbit anti-P-p65 (Ser 536), rabbit anti-β-Tubulin, rabbit anti-GAPDH, rabbit anti-FAK (Tyr 397) (Cell Signaling Technologies), rabbit anti-integrin α5, rabbit anti-integrin αv, rabbit anti-ILK, rabbit anti-VCAM1, rabbit anti-ICAM1, rabbit anti-β1 integrin (9G7) (BD Pharmingen) (**Supplemental Table I**). The following day after rinsing with TBST, HRP-conjugated secondary antibodies (Jackson ImmunoResearch) in blocking buffer were applied for two hours. Antibodies were detected using Pierce ECL solution (ThermoFisher) and x-ray film (Phenix Research Products).

Immunocytochemistry- Cells were plated on coverslips or slides and fixed in formaldehyde and permeabilized using 0.2% Triton X100 solution. Coverslips-containing cells were blocked with 10% horse serum for an hour. Subsequently, cells were washed and incubated with primary antibodies overnight (**Supplemental Table I**). Next, fluorochrome-tagged secondary antibodies (Life Technologies) were added to coverslips for 2 hours. After rinsing, cells were counterstained with DAPI. We used Nikon Eclipse Ti inverted epifluorescence microscope equipped with a Photometrics CoolSNAP120 ES2 camera and the NIS Elements 3.00, SP5 imaging software.

Adhesion/spreading assay- Cells were plated sparsely on fibronectin-coated coverslips for 15, 30, or 60 minutes in serum-free DMEM. Next, cells were fixed with PBS-buffered, 4% formaldehyde and co-stained with 546-conjugated phalloidin and 9EG7 (active β1 integrin).

Integrin Activation Assay- Activation of $\alpha5\beta1$ integrins was assessed using a specific $\alpha5\beta1$ ligand mimetic as previously described. Briefly, after cells were stimulated, a glutathione S-transferase (GST) tagged portion of the FN protein (FN III 9-11) was added to the cell culture medium for 30 minutes. Cell were rinsed with fresh media and then lysed with 2X laemmli buffer, subjected to western blotting, and probed with rabbit anti-GST (~70kDa).

bioRxiv preprint doi: https://doi.org/10.1101/2020.02.14.949941; this version posted February 15, 2020. The copyright holder for this preprint (which was not certified by peer review) is the author/funder, who has granted bioRxiv a license to display the preprint in perpetuity. It is made available under aCC-BY-NC 4.0 International license.

Focal Adhesion Isolation- Endothelial cells were plated on glass slides and treated. After experiments, cells were exposed to hypertonic shock using triethanolamine (2.5 mmol/L at pH 7.0) for 3 minutes. Next, cell bodies were removed by pulsed hydrodynamic force (Conair WaterPIK) at ≈0.5 cms from and ≈90° to the surface of the slide scanning the entire length 3 times. Slides were visualized under a microscope to ensure complete removal of cell bodies before lysis in 2X Laemmli buffer.

Deoxycholate Solubility Assay- Fibronectin integrated into extracellular matrix is insoluble in a deoxycholate detergent. Discerning between the two pools of fibronectin (intracellular vs matricellular, ie. extracellular) was done using a deoxycholate solubility assay, as previously described[9] . Briefly, after stimulation, cells were rinsed with ice cold PBS, incubated with DOC buffer (2% Sodium Deoxycholate, 20mM Tris-HCL, pH 8.8, 2 mM PMSF, 2mM Iodoacetic Acid (IAA), 2mM N-ethylmaleimide (NEM), 10mM EDTA, pH 8), lysed, and then passed through a 25G needle. The DOC-insoluble matrix fraction was pelleted by centrifugation, and the DOC-soluble supernatant fraction was collected. After rinsing the pellet with additional DOC buffer, the DOC-insoluble faction was lysed in a solubilization buffer (2% SDS, 25mM Tris-HCL, pH 8, 2mM PMSF, 2mM Iodoacetic Acid (IAA), 2mM N-ethylmaleimide (NEM), 10mM EDTA, pH 8). Samples were subjected to western blotting and probed with rabbit anti-fibronectin.

Quantitative real-time PCR- qRT-PCR was done as previously described[12]. Briefly, mRNA was extracted from tissues using TRIzol (Life Technologies, Inc., Carlsbad, CA). Next, iScript cDNA synthesis kit (Bio-Rad, Hercules, CA) was used to synthesize Complimentary DNA. qRT-PCR was done using Bio-Rad iCycler with the use of SYBR Green Master mix (Bio-Rad). We used the online Primer3 software and verified by sequencing the PCR products (**Supplemental Table I**). Results were expressed as fold change by using the 2-ΔΔCT method.

LDL Oxidation- Low density lipoprotein was purchased from Alfa Aesar and oxidized using 13.8 mM copper sulfate as previously described[8]. Briefly, LDL was dialyzed in 1xPBS for 24 hours, then oxidized in 1xPBS containing 13.8 mM copper sulfate for 24 hours followed with 50 µmol/L EDTA in 1x PBS for another day. Nitrogen gas was infused over oxLDL prior to storage, and oxLDL was tested for endotoxin contamination using a chromogenic endotoxin quantification kit (Thermo Scientific).

Animals and Tissue Harvesting- The Louisiana State University Health Sciences Center-Shreveport Animal Care and Use Committee approved all animal protocols, and all animals were cared for according to the National Institutes of Health Guide for the Care and Use of Laboratory Animals. C57Bl/6J mice with a tamoxifen inducible, VE-cadherin-CreERT2 transgene (from Ralf Adams, Max Planck, Germany) with either wildtype talin1, floxed alleles for talin1, or with an L325R mutation in talin1[27]. All mice were backcrossed to C57BL/6J mice for at least 7 generations. At 8 weeks of age, mice were treated with 1 mg/kg tamoxifen (Sigma-Aldrich, St Louis, MO) via intraperitoneal injection every day for 5 total injections to induce Cre expression and gene excision. Four weeks after tamoxifen injection, mice underwent partial carotid ligation as previously described[28] . Briefly, a superficial midline incision on the neck of mice under isoflurane anesthesia was done to expose the left carotid artery. Two 7-0 silk sutures were used to tie-off (occlude flow) to the internal, external, and occipital branches of the left carotid artery, whereas flow remained patent through the superior thyroid artery branch. The incision was closed with surgical glue and 6-0 silk sutures. Carprofen (5mg/kg) was administered as a post-surgical analgesic and 800uL of saline solution was given subdurally to prevent dehydration stress. Surgical success was confirmed via echocardiography 1 to 2 days prior to endpoint for

bioRxiv preprint doi: https://doi.org/10.1101/2020.02.14.949941; this version posted February 15, 2020. The copyright holder for this preprint (which was not certified by peer review) is the author/funder, who has granted bioRxiv a license to display the preprint in perpetuity. It is made available under aCC-BY-NC 4.0 International license.

confirmation of ligation. Mice were euthanized by pneumothorax under isoflurane anesthesia for tissue collection either 2- or 7-days post-surgery. After 2 days, carotid arteries were collected for RNA isolation performed by a TRIzol flush as previously described[28] . Briefly, carotids were cleaned of perivascular adipose tissue and flushed with 150 mL TRIzol from an insulin syringe. The remaining media/adventitia were then placed in 150 mL TRIzol and sonicated to lyse the tissue. Samples were then frozen until analysis by quantitative PCR. After 7 days, the carotids were excised, placed in 4% PBS buffered formaldehyde, and processed for immunohistochemistry.

Immunohistochemistry- Tissue was fixed in PBS-buffered, 4% formaldehyde, processed for paraffin embedding, and cut into 5 μm thick sections onto superfrost plus glass sides. After heated and subjected sodium citrate antigen retrieval (Vector Labs, H-3300), tissue was blocked using 10% horse serum, 1% BSA in PBS. Primary antibodies were applied overnight, followed by Alexa Fluor conjugated secondary antibodies (Thermo Fisher). Stains are imaged on a Nikon Eclipse Ti inverted fluorescent microscope. Images are captured at either a 10X, 20X, or 60X (oil objective) using the Photometrics Coolsnap120 ES2 camera and the NIS Elements BR 3.00, SP5 imaging software. NF-κB nuclear translocation was visualized by Leica TCS SP5 confocal microscope using 63X (oil objective) and the Nikon NIS-Elements C software.

Statistical analysis- Statistical analysis was performed using GraphPad Prism software. All of the data were tested for normality using Kolmogorov-Smirnov test. Data passing the normality tests were analyzed using either Student's t-test, 1-way ANOVA with Newman-Keuls post-test, or 2-way ANOVA with Bonferroni post-tests depending upon the number of independent variables and groups. Data failing the normality test were analyzed using the nonparametric Mann-Whitney U test and the Kruskal-Wallis test with post hoc analysis.

Results

Talin1 L325R mutant endothelial cells lack oxLDL and flow-induced α5β1 integrin activation. To characterize the role of integrin activation in endothelial cell function, we isolated mouse lung endothelial cells from Talin1$^{fl/L325R}$ mice that express one floxed talin1 allele and one L325R mutant allele. Talin1$^{fl/L325R}$ endothelial cells were then treated with adenovirus expressing either GFP (talin1 wildtype (WT)) or expressing Cre recombinase (talin1 L325R) to delete the floxed allele. While the talin1 L325R endothelial cells contain only one copy of the talin1 gene, Talin1 WT and L325R endothelial cells show equivalent protein levels of talin1 (**Figure 1A**). Talin1 L325R endothelial cells show slowed adhesion and spreading compared to talin1 WT cells. However, talin1 mutant cells eventually adhere, spread, and form a monolayer (**Figure 1B**), suggesting endothelial cell adhesion and spreading under static conditions do not require the high affinity integrin confirmation. Using immunostaining and isolated focal adhesion fractions, we observed that both talin1 WT and talin1 L325R endothelial cells show recruitment of talin1 and active β1 integrins (9EG7 antibody) into focal adhesions (**Figure 1C/D**). While levels of talin1 and α5β1 were slightly reduced in talin1 L325R cells **(Figure 1C)**, other components of the focal adhesion (paxillin, vinculin) show similar recruitment in talin1 WT and talin1 L325R endothelial cells **(Supplemental Figure I**), consistent with the retained ability of talin1 L325R to support cell adhesion and spreading.

bioRxiv preprint doi: https://doi.org/10.1101/2020.02.14.949941; this version posted February 15, 2020. The copyright holder for this preprint (which was not certified by peer review) is the author/funder, who has granted bioRxiv a license to display the preprint in perpetuity. It is made available under aCC-BY-NC 4.0 International license.

The presence of only the Talin1 L325R mutant impairs αIIbβ3 activation in platelets[22] and αLβ2 activation in leukocytes[23]. Therefore, we assessed whether talin1 L325R endothelial cells show a similar reduction in α5β1 integrin activation in response to flow and oxLDL[8,25]. Talin1 WT and L325R endothelial cells were exposed to shear stress or oxLDL, and α5β1 activation was measured using the ligand mimetic GST-FNIII$_{9\text{-}11}$, a GST fusion protein containing 9th to 11th type III repeats of fibronectin[25]. Retention of GST-FNIII$_{9\text{-}11}$ is specifically mediated by $\alpha5\beta1$ and is sensitive the both positive and negative regulators of integrin activation[25]. While basal levels of $\alpha5\beta1$ activity were similar between talin1 WT and talin1 L325R endothelial cells (**Figure 2A/B**), the enhanced α5β1 activation observed in response to shear stress (**Figure 2A**), and oxLDL (**Figure 2B**) was absent in talin1 L325R endothelial cells. Immunostaining for active β1 (9EG7) showed enhanced active β1 staining in response to oxLDL and flow in talin1 WT but not talin1 L325R endothelial cells, consistent with a deficiency in integrin activation (**Figure 2C/D**). These results provide the first evidence that talin1 is dispensable for basal integrin activation, cell adhesion, and spreading but required for inducible integrin activation in endothelial cells.

Talin1 L325R mutation blocks endothelial inflammation on fibronectin. At atherosclerosis prone regions, NF-κB signaling plays a major role in driving endothelial activation[4]. Signaling through α5β1 mediates NF-κB activation and enhanced proinflammatory gene expression in response to both oxLDL[8,9] and shear stress[16,29-32]. Since integrin inhibitors (small molecule inhibitors, blocking antibodies) blunt shear stress and oxLDL-induced NF-κB activation, we and others have postulated that new integrin-matrix interactions likely drive endothelial responses to both stimuli. However, these inhibitors may also compete with pre-existing integrin-matrix interactions. Therefore, we utilized talin1 WT and L325R endothelial cells to study the specific role of integrin activation in response to shear stress and oxLDL. Whereas both oxLDL and shear stress induce phosphorylation of the NF-κB p65 subunit (hereafter NF-κB), neither oxLDL nor shear stress induced significant NF-κB phosphorylation in talin1 L325R endothelial cells **(Figure 3A/B)**. Similarly, NF-κB nuclear translocation in response to oxLDL and shear stress was observed in talin1 WT but not talin1 L325R endothelial cells (**Figure 3C/D**). In contrast, other known shear-responsive signaling events, such as activation of ERK1/2, AKT, and eNOS (**Supplemental Figure II**) were activated similarly in talin1 WT and talin1 L325R endothelial cells, indicating these signaling responses are independent of shear stress-induced integrin activation[33]. Since α5β1 mediates oxLDL and flow-induced proinflammatory gene expression, we examined the effect of blocking talin1-dependent integrin activation in this response. Consistent with the suppressed NF-κB activation, our results show a marked inhibition of VCAM-1 and ICAM-1 in response to chronic oscillatory shear stress (OSS) (**Figure 4A/B**) and oxLDL (**Figure 4C/D**) in talin1 L325R endothelial cells. However, talin1-depenent integrin activation is not required for endothelial VCAM-1 expression in response to TNFα, IL-1β and LPS **(Figure 4E**), consistent with a specific role for integrin signaling in oxLDL and flow-induced endothelial activation.

Aberrant fibronectin fibrillogenesis in endothelial cells expressing Talin1 L325R mutation. In addition to inflammation, α5β1 integrins regulate fibronectin deposition in response to oxLDL and shear stress[9,32]. However, it is unclear whether basal integrin activation or inducible integrin activation is required to mediate fibronectin matrix deposition. Therefore, we sought to examine the role of fibronectin deposition in talin1 L325R mutant endothelial cells. Talin1 WT and talin1 L325R endothelial cells were plated on basement membrane proteins for 4 hours and then were exposed to either disturbed flow or oxLDL for 24 hours. Fibronectin deposition into the deoxycholate-insoluble matrix fraction was compared using Western blotting and immunocytochemistry as previously described[9]. Talin1 WT endothelial cells showed a low level

bioRxiv preprint doi: https://doi.org/10.1101/2020.02.14.949941; this version posted February 15, 2020. The copyright holder for this preprint (which was not certified by peer review) is the author/funder, who has granted bioRxiv a license to display the preprint in perpetuity. It is made available under aCC-BY-NC 4.0 International license.

of fibronectin deposition under unstimulated conditions that increased significantly in response to both oscillatory shear stress (OSS) (**Figure 5A**) and oxLDL (**Figure 5B**). However, talin1 L325R endothelial cells failed to deposit fibronectin in response to either stimulus. To gain further insight into this response, the fibronectin matrix was visualized by immunocytochemistry. As previously show, both OSS and oxLDL increased fibronectin staining in the subendothelial matrix (**Figure 5C/D**), associated with both increased fluorescence intensity for fibronectin (**Figure 5E/F**) and increased fibronectin fibril length (**Figure 5G/H**). However, OSS and oxLDL both failed to induce fibronectin staining intensity or enhance fibronectin fibril length in talin1 L325R endothelial cells.

Although the talin1 L325R endothelial cells were deficient for fibronectin deposition, fibronectin expression was similar between the talin1 WT and talin1 L325R endothelial cells (**Supplemental Figure III**), suggesting the defect may be in matrix deposition. Fibronectin fibril assembly involves α5β1 translocation from peripheral focal adhesions into tensin1-rich fibrillar adhesions that organize the fibronectin dimers into higher order fibrils[9,34]. To assess whether talin1-dependent integrin activation affects the formation of fibrillar adhesions, talin1 WT and talin1 L325R endothelial cells were treated with oxLDL or OSS, and the composition of endothelial adhesions was assessed by immunocytochemistry and Western blotting analysis of the isolated focal adhesion fraction. Both oxLDL and OSS stimulated enhanced recruitment of α5 integrins into the focal adhesions in talin1 WT endothelial cells (**Figure 6A/B**), consistent with an increase in fibrillar adhesion formation. However, focal adhesion levels of α5 were static in talin1 L325R endothelial cells. Similarly, both oxLDL and OSS promoted focal adhesion recruitment of tensin1 in talin1 WT but not talin1 L325R endothelial cells (**Figure 6C/D**). Together, these data suggest that inducible integrin activation and the formation of new cell-matrix interactions are critical for fibrillar adhesion development and fibronectin deposition in endothelial cells.

Requirement of integrin signaling for endothelial activation and matrix remodeling.
While these data indicate that a subset of endothelial responses to oxLDL require inducible integrin activation, it remains unclear whether integrin activation and signaling are sufficient for these responses. To test the relative role of integrin activation in endothelial proinflammatory gene expression and fibronectin deposition, we employed CHAMP peptides targeted to the α5 integrin transmembrane region to selectively activate $\alpha5\beta1$ in the integrin activation-deficient talin1 L325R cells. Treatment with the α5 CHAMP peptide was partially sufficient to induce fibronectin deposition in talin1 L325R endothelial cells **(Figure 6A/B)**, which was fully recovered by treatment with a combination of α5 CHAMP peptides and oxLDL **(Figure 6A/B)**. While α5 is clearly required for oxLDL-induced NF-κB activation[8], activation of $\alpha5\beta1$ with the α5 CHAMP peptide was not sufficient to induce NF-κB activation **(Figure 6C)**. However, simultaneous treatment with both oxLDL and the α5 CHAMP peptide restored NF-κB activation in talin1 L325R endothelial cells **(Figure 6C)**, suggesting that NF-κB activation in response to oxLDL requires both integrin-dependent and integrin-independent signaling pathways. Taken together, these data suggest that oxLDL-induced $\alpha5\beta1$ integrin activation alone can mediate fibronectin assembly, whereas NF-κB activation and maximal fibronectin assembly requires co-stimulatory integrin-dependent and integrin-independent signaling pathways.

Mice expressing endothelial talin1 L325R are protected from atherogenic inflammation. Since our *in vitro* studies show a clear role for talin1-dependent integrin activation in atherogenic endothelial activation, we next examined whether mice expressing only talin1 WT or talin1 L325R in their endothelial cells show differential susceptibility to disturbed flow-induced endothelial activation *in vivo*. Tamoxifen-inducible, endothelial-specific talin1 WT (iEC-Talin1 WT;

bioRxiv preprint doi: https://doi.org/10.1101/2020.02.14.949941; this version posted February 15, 2020. The copyright holder for this preprint (which was not certified by peer review) is the author/funder, who has granted bioRxiv a license to display the preprint in perpetuity. It is made available under aCC-BY-NC 4.0 International license.

Talin1$^{WT/flox}$, VE-Cadherin-CreERT$^{tg/?}$) and talin1 L325R (iEC-Talin1 L325R; Talin1$^{flox/L325R}$, VE-Cadherin-CreERT$^{tg/?}$) mice underwent partial ligation of the left carotid artery to induce low, oscillatory flow. The right carotid artery remained exposed to laminar flow and was used as an internal control. After 48 hours, intimal mRNA was isolated to analyze endothelial proinflammatory gene expression using qRT-PCR. Intimal mRNA preparations were shown to be enriched for CD31 and deficient in smooth muscle actin compared to medial mRNA (**Figure 8A**). Both iEC-Talin1 WT and iEC-Talin1 L325R mice show reduced KLF2 expression in the left carotid artery following partial ligation, consistent with a loss of laminar flow (**Figure 8B**). However, only iEC-Talin1 WT mice showed a significant increase in proinflammatory gene expression (ICAM-1, VCAM-1) in the left carotid, whereas iEC-Talin1 L325R mice showed no upregulation of proinflammatory gene expression (**Figure 8B**). In addition to mRNA analysis, we harvested carotid arteries from iEC-Talin1 WT and iEC-Talin1 L325R mice 7 days after partial carotid ligation for immunohistochemical analysis. Consistent with our *in vitro* data, iEC-Talin1 L325R mice show a remarkable reduction of endothelial NF-κB nuclear translocation (**Figure 8C/D**), VCAM-1 expression (**Figure 8E/F**), and macrophage (Mac2-positive) recruitment (**Figure 8G/H**). In contrast, carotid endothelial (CD31-positive) and smooth muscle (smooth muscle actin-positive) content was similar between iEC-Talin1 WT and iEC-Talin1 L325R mice (**Supplemental Figure IV**). Altogether, these data show for the first time that modulating integrin affinity in endothelial cells contributes to endothelial phenotype both *in vitro* and *in vivo*.

Discussion

Cell-matrix interactions play a critical role in endothelial activation and early atherosclerosis[2], however, the role of integrin activation in this context remains enigmatic. Previously, we showed that fibronectin enhances proinflammatory responses to flow and oxLDL and deleting fibronectin-binding integrins in the endothelium blunts atherogenic inflammation[8,9]. Using mice expressing L325R Talin1 mutation that selectively inhibits integrin activation without affecting basal cell adhesion and spreading, we demonstrate for the first time that talin1-dependent integrin activation is crucial for endothelial inflammation to drive atherosclerosis. Specifically, we showed that talin1 is critical for α5 integrin activation in response to oxLDL and flow without affecting the structure of focal adhesions. We further show that talin1-dependent integrin activation is critical for fibronectin deposition, NF-κB activation, and proinflammatory gene expression. Lastly, mice harboring a talin1 L325R mutation in endothelial cells show a significant reduction in proinflammatory gene expression and macrophage accumulation in the partial carotid ligation model of disturbed flow.

While talin1 is required for leukocyte and platelet adhesion, talin1 is dispensable for initial cell adhesion and spreading in endothelial cells. Like endothelial cells, talin1-deficient fibroblasts adhere and spread normally, presumably due to overexpression of talin2[35]. While endothelial cells typically only express talin1[36], overexpression of talin2 may compensate for talin1 loss to support endothelial cell adhesion and spreading[20,36-38]. However, talin1 L325R mutant endothelial cells show impaired integrin activation in response to oxLDL and flow, indicating that talin2 is not sufficient to drive inducible integrin activation in endothelial cells. Integrins exist in multiple activation states, including a bent, closed state (inactive), an intermediate extended state with a closed headpiece (partially active), and a fully extended, open conformation (active)[39] . In neutrophils lacking talin1 or expressing a talin1 W359A mutation that prevents binding of talin1 to the β integrin subunit, neutrophils show defective chemokine-induced, β2 integrin–mediated slow

bioRxiv preprint doi: https://doi.org/10.1101/2020.02.14.949941; this version posted February 15, 2020. The copyright holder for this preprint (which was not certified by peer review) is the author/funder, who has granted bioRxiv a license to display the preprint in perpetuity. It is made available under aCC-BY-NC 4.0 International license.

rolling, arrest, spreading, and migration[23]. In contrast, talin1 L325R expressing neutrophils support partial activation of β2 integrins resulting in a normal slow rolling response but defective firm adhesion[23]. Therefore, the presence of talin1 L325R in endothelial cells may allow the endothelial cell integrins to attain the partially activated confirmation, thereby supporting cell adhesion and spreading in the mild mechanical environment of static cell culture.

Integrins are involved in a vast spectrum of biological processes, including cell adhesion, gene expression, proliferation, and cell migration[40]. Deletion of fibronectin or fibronectin-binding integrins (α5β1, αvβ3) limits endothelial NF-κB activation and proinflammatory gene expression in atherosclerosis models[9,11], whereas β1 integrin inhibition reduces vascular permeability in response to proinflammatory mediators (LPS, IL-1β)[41]. To dissect the role of integrin signaling in endothelial cell phenotype, several groups have used variety of integrin inhibitors and blocking antibodies to implicate integrin activation and new integrin-matrix interactions in endothelial proinflammatory responses, particularly in response to flow and oxLDL[8,12] . However, integrin inhibitors and blocking antibodies have the potential to affect pre-existing integrin-matrix interactions as well, making it difficult to determine the specific role of integrin activation and new integrin-matrix interactions. In addition, the use of ligand-mimetic inhibitors may stimulate ligation-dependent signaling, and anti-integrin antibodies may induce a subset of integrin signaling due to clustering. Our model of talin1 L325R mutant endothelial cells eliminates these barriers by specifically eliminating talin1-dependent integrin activation without affecting talin1-dependent focal adhesion formation. The talin1 L325R mutant endothelial cells provide the first conformation of an important role for endothelial integrin activation in fibronectin deposition, NF-κB activation, and proinflammatory adhesion molecule expression (VCAM-1, ICAM-1).

Previous studies in mouse models clearly implicate cell-matrix interactions in atherogenic endothelial activation but fail to connect endothelial integrin activation to these responses. The endothelial-specific talin1 L325R mutant mouse is the first model that directly tests the role of endothelial integrin affinity modulation *in vivo*. Interestingly, endothelial talin1 knockout mice show destabilized endothelial cell-cell junctions, mostly due to disruption of vascular endothelial-cadherin organization. While talin1 reexpression restores endothelial adherens junction structure, rescuing integrin activation with the talin1 head domain (but not a L325R head domain mutant) only partially reverts this phenotype. These data suggest an important role for both talin1-dependent integrin activation and talin1-mediated actin binding in maintaining vascular barrier function[21]. Similarly, β1 integrin expression is crucial for the development of stable, non-leaky vessels[42]. However, inhibiting β1 integrins limits LPS-induced vascular leakage, suggesting that integrin signaling may play differential roles in regulating vascular permeability in developing blood vessels compared to mature vessels.

Much of our current understanding of integrin activation derives from studies in platelets and leukocytes, leading to the development of a multiple therapeutics for hematological and cardiovascular diseases. However, far less is known concerning integrin activation in adherent cell types, such as the endothelium. These studies demonstrate for the first time a vital role for endothelial integrin activation in the regulation of endothelial phenotype and proinflammatory gene expression *in vitro* and *in vivo*. Specifically, we provide the first evidence that talin1-dependent integrin activation drives endothelial proinflammatory responses *in vitro*, and selectively blocking integrin activation in endothelial cells reduces endothelial proinflammatory responses to disturbed flow *in vivo*. Through a better understanding of the molecular mechanisms

bioRxiv preprint doi: https://doi.org/10.1101/2020.02.14.949941; this version posted February 15, 2020. The copyright holder for this preprint (which was not certified by peer review) is the author/funder, who has granted bioRxiv a license to display the preprint in perpetuity. It is made available under aCC-BY-NC 4.0 International license.

regulating endothelial integrin activation, we may be able to generate future therapeutics that limit endothelial integrin activation to reduce inflammation in a variety of pathological contexts.

Acknowledgements:
None.

Source of Funding:
This work was supported by National Heart, Lung, and Blood Institute R01 HL098435, HL133497, HL141155, and GM121307 (to A.W.O.), by an American Heart Association Pre-doctoral Fellowship (19PRE34380751) and Malcolm Feist Cardiovascular Research Endowment Pre-doctoral Fellowship (to Z.A.Y.).

Disclosures:
The authors declare no conflicts.

bioRxiv preprint doi: https://doi.org/10.1101/2020.02.14.949941; this version posted February 15, 2020. The copyright holder for this preprint (which was not certified by peer review) is the author/funder, who has granted bioRxiv a license to display the preprint in perpetuity. It is made available under aCC-BY-NC 4.0 International license.

References:

1. Pober, J.S. & Sessa, W.C. Evolving functions of endothelial cells in inflammation. *Nat Rev Immunol* **7**, 803-15 (2007).
2. Yurdagul, A., Jr. & Orr, A.W. Blood Brothers: Hemodynamics and Cell-Matrix Interactions in Endothelial Function. *Antioxid Redox Signal* **25**, 415-34 (2016).
3. Collins, T. & Cybulsky, M.I. NF-kappaB: pivotal mediator or innocent bystander in atherogenesis? *Journal of Clinical Investigation* **107**, 255-64 (2001).
4. Hajra, L. *et al.* The NF-kappa B signal transduction pathway in aortic endothelial cells is primed for activation in regions predisposed to atherosclerotic lesion formation. *Proc Natl Acad Sci U S A* **97**, 9052-7 (2000).
5. Orr, A.W. *et al.* The subendothelial extracellular matrix modulates NF-kappaB activation by flow: a potential role in atherosclerosis. *J Cell Biol* **169**, 191-202 (2005).
6. Feaver, R.E., Gelfand, B.D., Wang, C., Schwartz, M.A. & Blackman, B.R. Atheroprone hemodynamics regulate fibronectin deposition to create positive feedback that sustains endothelial inflammation. *Circ Res* **106**, 1703-11 (2010).
7. Green, J., Yurdagul, A., Jr., McInnis, M.C., Albert, P. & Orr, A.W. Flow patterns regulate hyperglycemia-induced subendothelial matrix remodeling during early atherogenesis. *Atherosclerosis* **232**, 277-84 (2014).
8. Yurdagul, A., Jr. *et al.* alpha5beta1 integrin signaling mediates oxidized low-density lipoprotein-induced inflammation and early atherosclerosis. *Arterioscler Thromb Vasc Biol* **34**, 1362-73 (2014).
9. Al-Yafeai, Z. *et al.* Endothelial FN (Fibronectin) Deposition by alpha5beta1 Integrins Drives Atherogenic Inflammation. *Arterioscler Thromb Vasc Biol* **38**, 2601-2614 (2018).
10. Hynes, R.O. Integrins: bidirectional, allosteric signaling machines. *Cell* **110**, 673-87 (2002).
11. Rohwedder, I. *et al.* Plasma fibronectin deficiency impedes atherosclerosis progression and fibrous cap formation. *EMBO Mol Med* **4**, 564-76 (2012).
12. Chen, J. *et al.* alphavbeta3 Integrins Mediate Flow-Induced NF-kappaB Activation, Proinflammatory Gene Expression, and Early Atherogenic Inflammation. *Am J Pathol* **185**, 2575-89 (2015).
13. Finney, A.C., Stokes, K.Y., Pattillo, C.B. & Orr, A.W. Integrin signaling in atherosclerosis. *Cell Mol Life Sci* **74**, 2263-2282 (2017).
14. Pickering, J.G. *et al.* alpha5beta1 integrin expression and luminal edge fibronectin matrix assembly by smooth muscle cells after arterial injury. *Am J Pathol* **156**, 453-65 (2000).
15. Cai, W.J. *et al.* Activation of the integrins alpha 5beta 1 and alpha v beta 3 and focal adhesion kinase (FAK) during arteriogenesis. *Mol Cell Biochem* **322**, 161-9 (2009).
16. Yun, S. *et al.* Interaction between integrin alpha5 and PDE4D regulates endothelial inflammatory signalling. *Nat Cell Biol* **18**, 1043-53 (2016).
17. Calderwood, D.A., Campbell, I.D. & Critchley, D.R. Talins and kindlins: partners in integrin-mediated adhesion. *Nat Rev Mol Cell Biol* **14**, 503-17 (2013).
18. Tadokoro, S. *et al.* Talin binding to integrin beta tails: a final common step in integrin activation. *Science* **302**, 103-6 (2003).
19. Wegener, K.L. *et al.* Structural basis of integrin activation by talin. *Cell* **128**, 171-82 (2007).
20. Monkley, S.J. *et al.* Endothelial cell talin1 is essential for embryonic angiogenesis. *Dev Biol* **349**, 494-502 (2011).
21. Pulous, F.E., Grimsley-Myers, C.M., Kansal, S., Kowalczyk, A.P. & Petrich, B.G. Talin-Dependent Integrin Activation Regulates VE-Cadherin Localization and Endothelial Cell Barrier Function. *Circ Res* **124**, 891-903 (2019).

bioRxiv preprint doi: https://doi.org/10.1101/2020.02.14.949941; this version posted February 15, 2020. The copyright holder for this preprint (which was not certified by peer review) is the author/funder, who has granted bioRxiv a license to display the preprint in perpetuity. It is made available under aCC-BY-NC 4.0 International license.

22. Stefanini, L. *et al.* A talin mutant that impairs talin-integrin binding in platelets decelerates alphaIIbbeta3 activation without pathological bleeding. *Blood* **123**, 2722-31 (2014).
23. Yago, T. *et al.* Blocking neutrophil integrin activation prevents ischemia-reperfusion injury. *J Exp Med* **212**, 1267-81 (2015).
24. Orr, A.W., Hahn, C., Blackman, B.R. & Schwartz, M.A. p21-activated kinase signaling regulates oxidant-dependent NF-kappa B activation by flow. *Circ Res* **103**, 671-9 (2008).
25. Orr, A.W., Ginsberg, M.H., Shattil, S.J., Deckmyn, H. & Schwartz, M.A. Matrix-specific suppression of integrin activation in shear stress signaling. *Mol Biol Cell* **17**, 4686-97 (2006).
26. Mravic, M. *et al.* De novo designed transmembrane peptides activating the alpha5beta1 integrin. *Protein Eng Des Sel* **31**, 181-190 (2018).
27. Haling, J.R., Monkley, S.J., Critchley, D.R. & Petrich, B.G. Talin-dependent integrin activation is required for fibrin clot retraction by platelets. *Blood* **117**, 1719-22 (2011).
28. Nam, D. *et al.* Partial carotid ligation is a model of acutely induced disturbed flow, leading to rapid endothelial dysfunction and atherosclerosis. *Am J Physiol Heart Circ Physiol* **297**, H1535-43 (2009).
29. Sun, X. *et al.* Activation of integrin alpha5 mediated by flow requires its translocation to membrane lipid rafts in vascular endothelial cells. *Proc Natl Acad Sci U S A* **113**, 769-74 (2016).
30. Yun, S. *et al.* Integrin alpha5beta1 regulates PP2A complex assembly through PDE4D in atherosclerosis. *J Clin Invest* **130**(2019).
31. Li, B. *et al.* c-Abl regulates YAPY357 phosphorylation to activate endothelial atherogenic responses to disturbed flow. *J Clin Invest* **129**, 1167-1179 (2019).
32. Budatha, M. *et al.* Inhibiting Integrin alpha5 Cytoplasmic Domain Signaling Reduces Atherosclerosis and Promotes Arteriogenesis. *J Am Heart Assoc* **7**(2018).
33. Tzima, E. *et al.* A mechanosensory complex that mediates the endothelial cell response to fluid shear stress. *Nature* **437**, 426-31 (2005).
34. Georgiadou, M., Lilja, J. & Jacquemet, G. AMPK negatively regulates tensin-dependent integrin activity. **216**, 1107-1121 (2017).
35. Zhang, X. *et al.* Talin depletion reveals independence of initial cell spreading from integrin activation and traction. *Nat Cell Biol* **10**, 1062-8 (2008).
36. Kopp, P.M. *et al.* Studies on the morphology and spreading of human endothelial cells define key inter- and intramolecular interactions for talin1. *Eur J Cell Biol* **89**, 661-73 (2010).
37. Lim, I.R. *et al.* Talin Modulation by a Synthetic N-Acylurea Derivative Reduces Angiogenesis in Human Endothelial Cells. *Int J Mol Sci* **18**(2017).
38. Gagat, M. & Grzanka, D. Letter by Gagat and Grzanka Regarding Article, "Talin-Dependent Integrin Activation Regulates VE-Cadherin Localization and Endothelial Cell Barrier Function". *Circ Res* **125**, e11-e12 (2019).
39. Shattil, S.J., Kim, C. & Ginsberg, M.H. The final steps of integrin activation: the end game. *Nat Rev Mol Cell Biol* **11**, 288-300 (2010).
40. Giancotti, F.G. & Ruoslahti, E. Integrin signaling. *Science* **285**, 1028-32 (1999).
41. Hakanpaa, L. *et al.* Targeting beta1-integrin inhibits vascular leakage in endotoxemia. *Proc Natl Acad Sci U S A* **115**, E6467-e6476 (2018).
42. Yamamoto, H. *et al.* Integrin β1 controls VE-cadherin localization and blood vessel stability.

bioRxiv preprint doi: https://doi.org/10.1101/2020.02.14.949941; this version posted February 15, 2020. The copyright holder for this preprint (which was not certified by peer review) is the author/funder, who has granted bioRxiv a license to display the preprint in perpetuity. It is made available under aCC-BY-NC 4.0 International license.

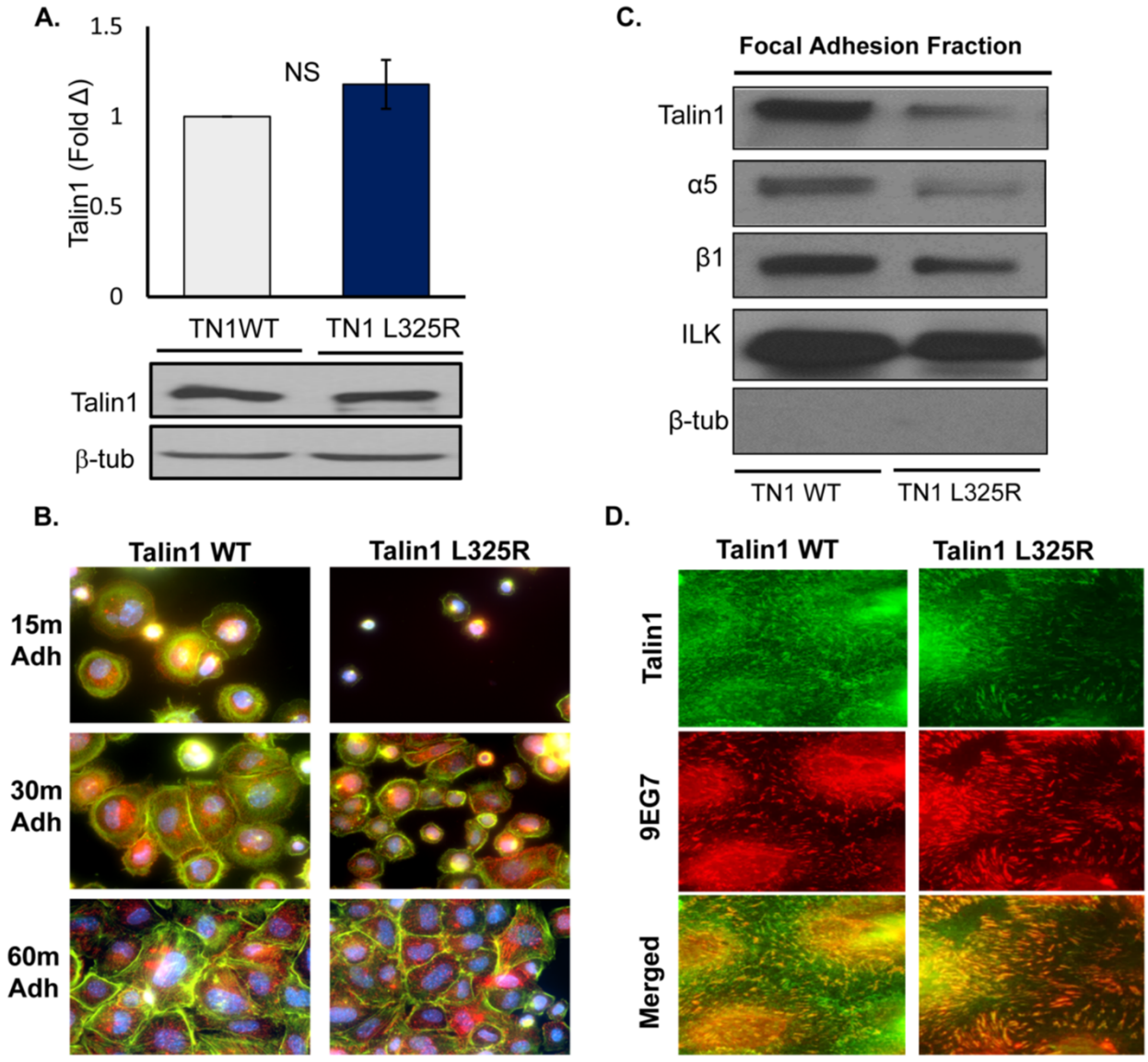

Figure 1. Talin1 L325R Endothelial Cells Show Normal Focal Adhesion Structure.. A) Representative western blots of Mouse Lung Endothelial Cells (MLEC) from different genotypes probed with Talin1 antibody showing equivalent levels of Talin1 in TN1 WT and TN1 L325R MLECs. B) Focal adhesion isolation (by hydrodynamic force) was conducted on TN1 WT and TN1 L325R MLECs plated overnight. The focal adhesion fractions were then blotted for different focal adhesion proteins. n=3. C) Talin1 WT and Talin1 L325R cells were plated on fibronectin for 15,30 and 60 minutes and then fixed and immunostained for 9EG7 (red), phalloidin 488 (green). D) Talin1 WT and Talin1 L325R MLECs were fixed and immunostained for Talin1 and 9EG7 (active β). Representative images are shown(n=3). n=3. Values are means ±SE. Student t test was used for statistical analysis.

bioRxiv preprint doi: https://doi.org/10.1101/2020.02.14.949941; this version posted February 15, 2020. The copyright holder for this preprint (which was not certified by peer review) is the author/funder, who has granted bioRxiv a license to display the preprint in perpetuity. It is made available under aCC-BY-NC 4.0 International license.

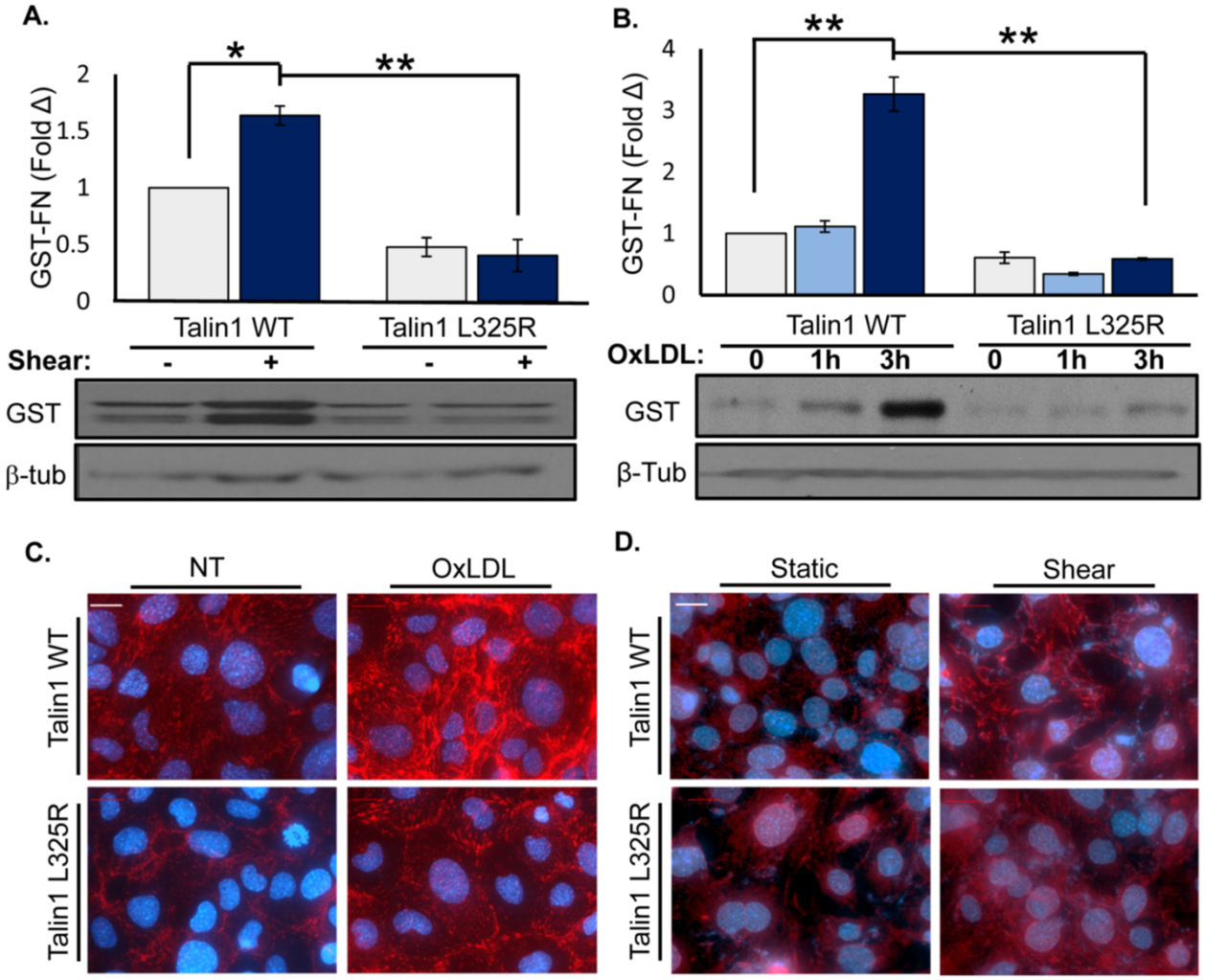

Figure 2. Talin1 Mediates Shear Stress and OxLDL (oxidized low-density lipoprotein)-Induced Integrin Activation. A/B) Talin1 WT and Talin1 L325R cells were plated on fibronectin and exposed to flow (5 minutes) or treated with oxLDL (100 ug/ml) for 1 or 3 hours. α5β1 activation was assessed by measuring GST-FNIII9-11 retention by western blot. n=4. C/D) Talin1 WT and Talin1 L325R cells were plated on fibronectin, then either treated with oxLDL (C) or exposed to shear stress (D) for 1 hour, then immunostaining for 9EG7 was performed. n=4-5. Values are means ±SE. *P<0.05 and **P<0.01 compared with 0 h time point. 2-way ANOVA with Bonferroni posttest (E-F) were used for statistical analyses.

bioRxiv preprint doi: https://doi.org/10.1101/2020.02.14.949941; this version posted February 15, 2020. The copyright holder for this preprint (which was not certified by peer review) is the author/funder, who has granted bioRxiv a license to display the preprint in perpetuity. It is made available under aCC-BY-NC 4.0 International license.

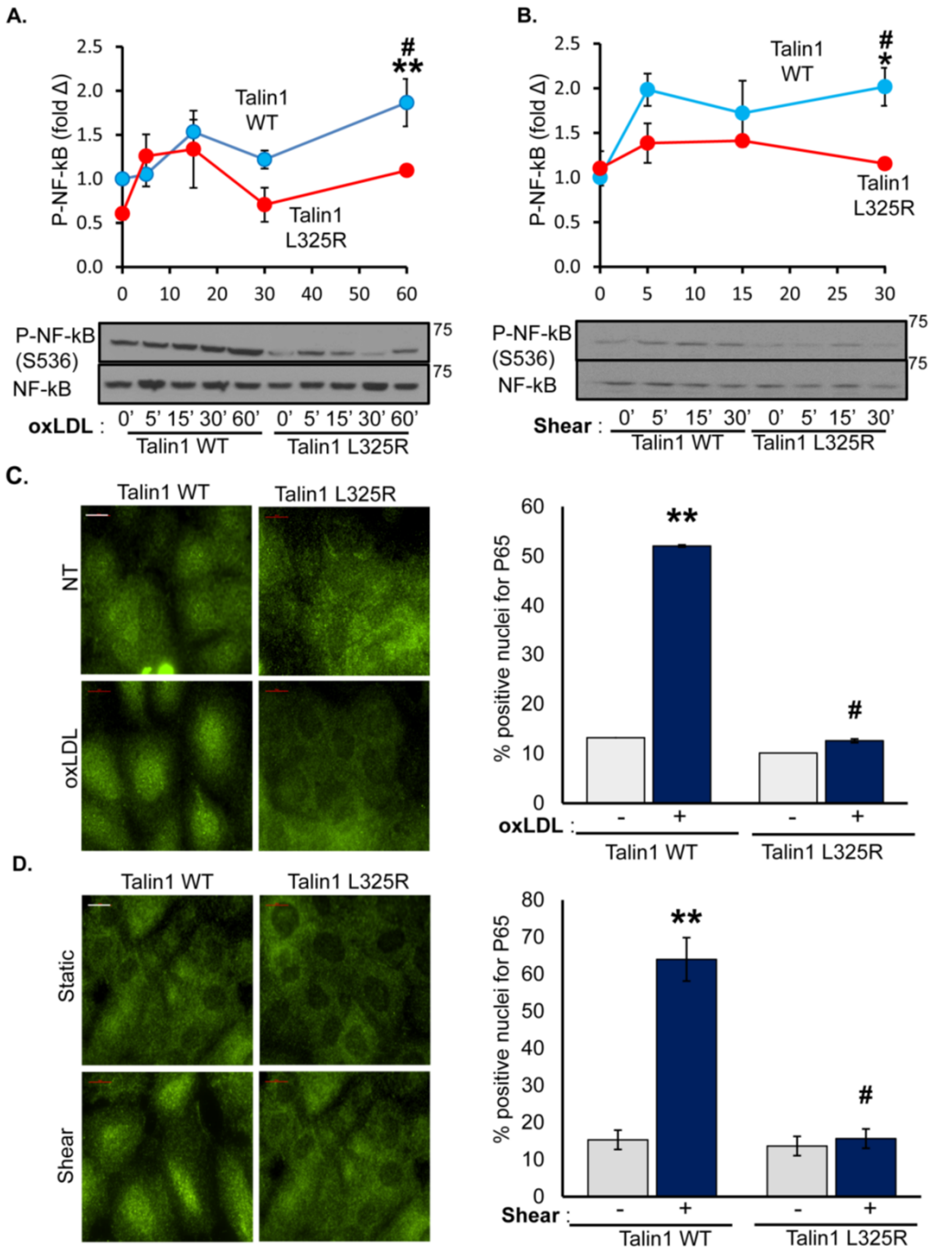

Figure 3. Blocking Talin1-Dependent Integrin Activation Blunts OxLDL (oxidized low-density lipoprotein) and Flow-Induced NF-κB Activation. A/B) Talin1 WT and Talin1 L325R cells were plated on fibronectin and treated with oxLDL or exposed to shear stress for the indicated time points. Western blotting was performed for P-NF-κB (p65, Ser536). Representative western blots are shown (n=4-5). B/D) Talin1 WT and Talin1 L325R cells were treated with oxLDL for an hour or flow for 30 minutes and then fixed and stained for NF-κB and positive nuclear translocation was quantified. Representative images are shown(n=4). D) Talin1 WT and Talin1 L325R cells were exposed to shear stress for the indicated times and P-NF-κB (p65, Ser536) was measured using western blot. Representative western blots are shown (n=4-5). Values are means ±SE. *P<0.05 and **P<0.001 compared *P<0.05 compared with 0 h time point. #P<0.05 compared with Talin1 L325R. 2-way ANOVA with Bonferroni posttest was used for statistical analyses.

bioRxiv preprint doi: https://doi.org/10.1101/2020.02.14.949941; this version posted February 15, 2020. The copyright holder for this preprint (which was not certified by peer review) is the author/funder, who has granted bioRxiv a license to display the preprint in perpetuity. It is made available under aCC-BY-NC 4.0 International license.

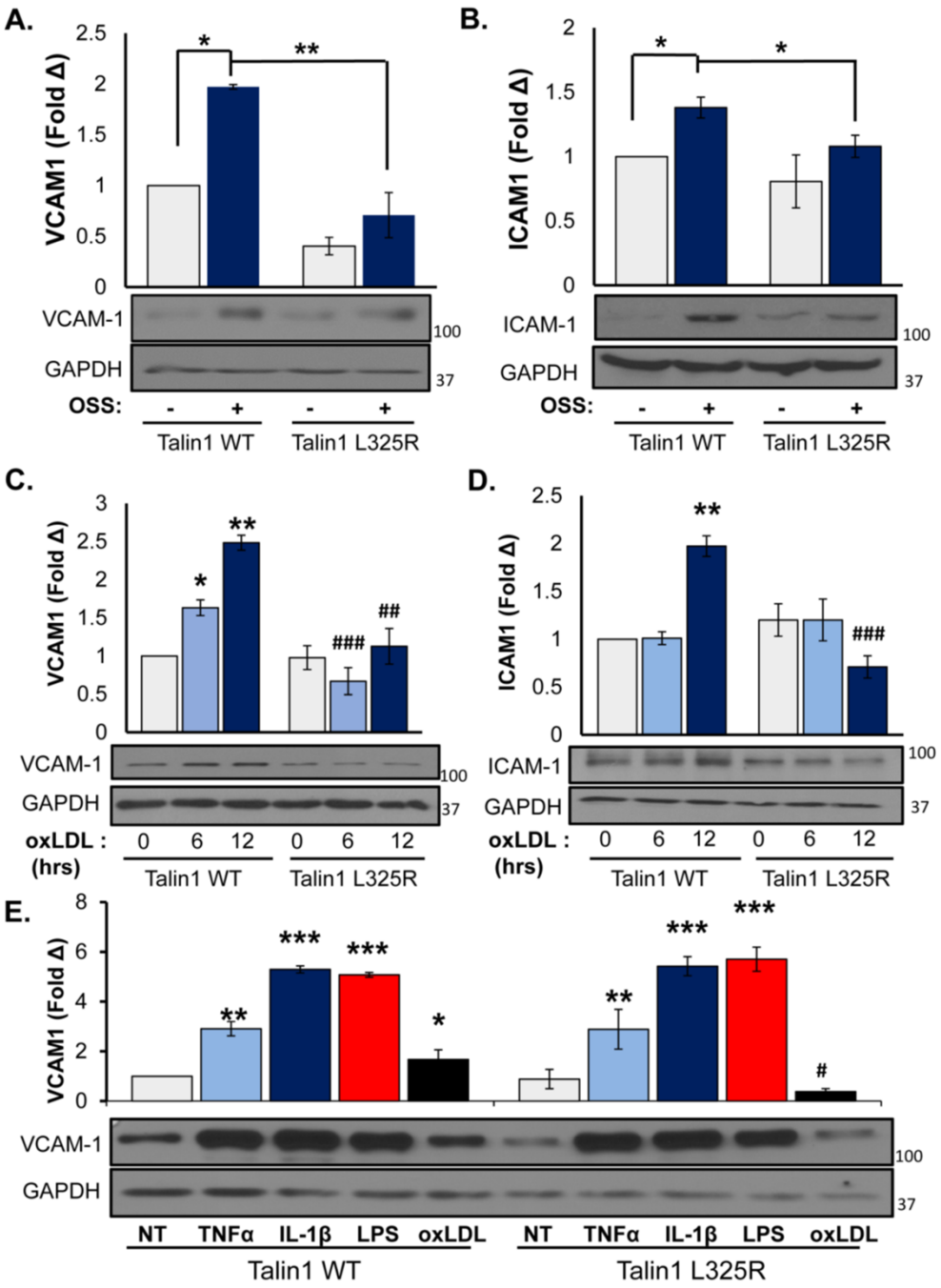

Figure 4. Talin1- Mediated Integrin Activation Is Required for OxLDL (oxidized low-density lipoprotein) and Flow-Induced Inflammation. A-B) Talin1 WT and Talin1 L325R MLECs (mouse Lung endothelial cells) were plated on fibronectin and exposed to oscillatory shear stress (OSS) for 18 hours. VCAM-1(vascular cell adhesion molecule-1) and ICAM-1(intercellular adhesion molecule-1) protein expression was measured using western blot. Representative western blots are shown (n=4-5). C-D) Talin1 WT and Talin1 L325R MLECs were treated with oxLDL for the indicated time points. Immunoblotting was conducted to assess VCAM-1 (C) and ICAM-1 (D) expression. Representative western blots are shown (n=4). D) Talin1 WT and Talin1 L325R MLECs were treated with TNFα (tumor necrosis factor α) (1 ug/ml), IL-1β (interleukin 1β) (5 ug /ml), LPS (lipopolysaccharide) (10 ug /ml), or oxLDL. VCAM-1 expression was assessed using western blot. Representative western blots are shown (n=3). Values are means ±SE. *P<0.05, **P<0.01 ***P<0.001 compared with 0 h time point. #P<0.05, ##P<0.01, and ###P<0.001 compared with Talin1 L325R. 2-way ANOVA with Bonferroni posttest was used for statistical analyses.

bioRxiv preprint doi: https://doi.org/10.1101/2020.02.14.949941; this version posted February 15, 2020. The copyright holder for this preprint (which was not certified by peer review) is the author/funder, who has granted bioRxiv a license to display the preprint in perpetuity. It is made available under aCC-BY-NC 4.0 International license.

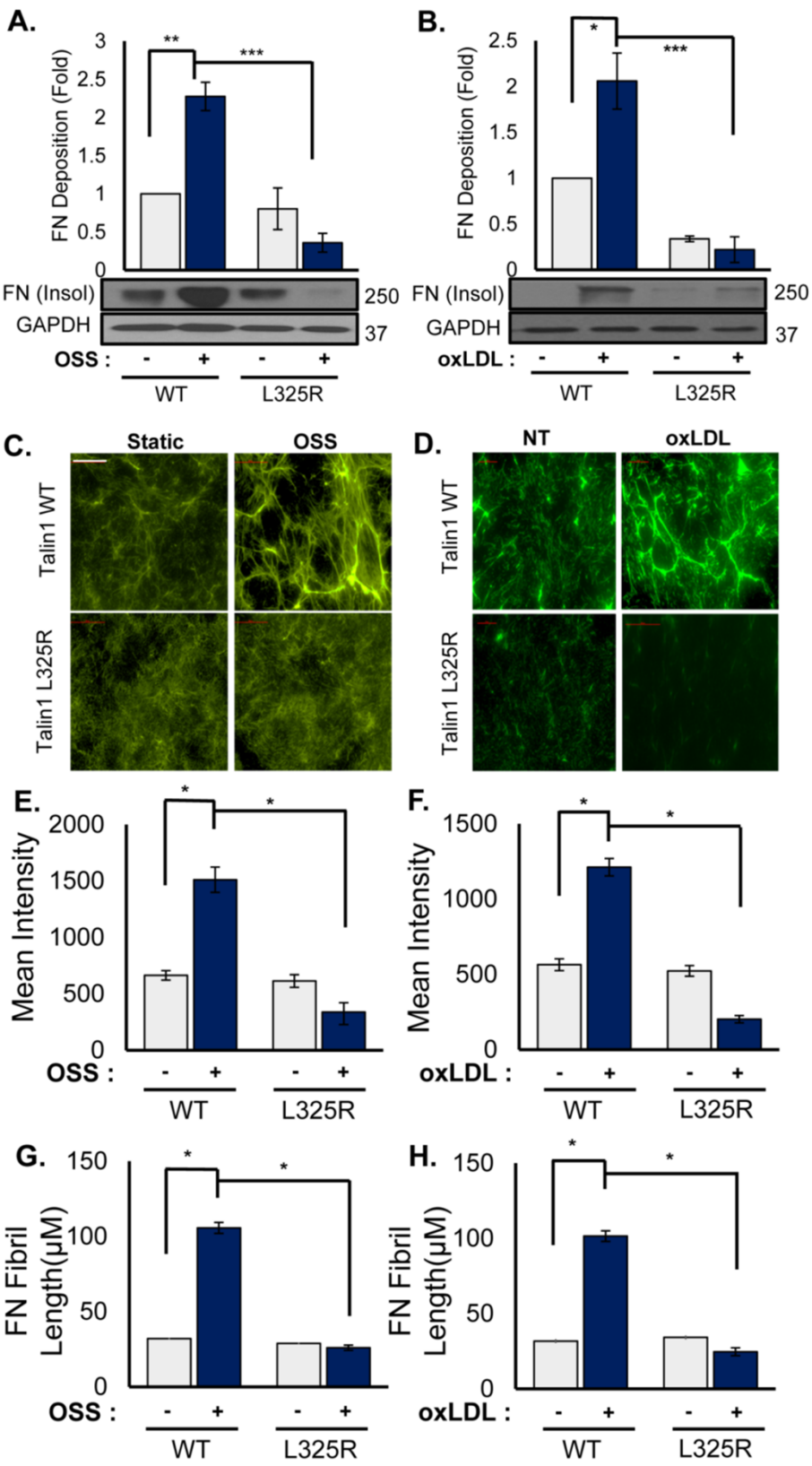

Figure 5. Talin1- Mediated Integrin Activation Promotes Fibronectin Fibrillogenesis. A/B) Talin1 WT and Talin1 L325R MLECs (mouse Lung endothelial cells) were plated on diluted Matrigel for 4 hours and then treated with oxLDL (oxidized low-density lipoprotein) or OSS (oscillatory shear stress) for 24 hours. Deoxycholate insoluble fractions were collected and western blot was conducted for fibronectin.=4. E-H) Talin1 WT and Talin1 L325R MLECs seeded on diluted Matrigel and treated with oxLDL or exposed to OSS for 24 hours. Immunocytochemistry was performed to test fibronectin deposition. Mean fluorescent intensity (E/F) and fibril length (G/H) were assessed. Representative images are shown(n=4-5). Values are means ±SE. *P<0.05, **P<0.01 ***P<0.001 compared with 0 h time point. 2-way ANOVA with Bonferroni posttest was used for statistical analyses.

bioRxiv preprint doi: https://doi.org/10.1101/2020.02.14.949941; this version posted February 15, 2020. The copyright holder for this preprint (which was not certified by peer review) is the author/funder, who has granted bioRxiv a license to display the preprint in perpetuity. It is made available under aCC-BY-NC 4.0 International license.

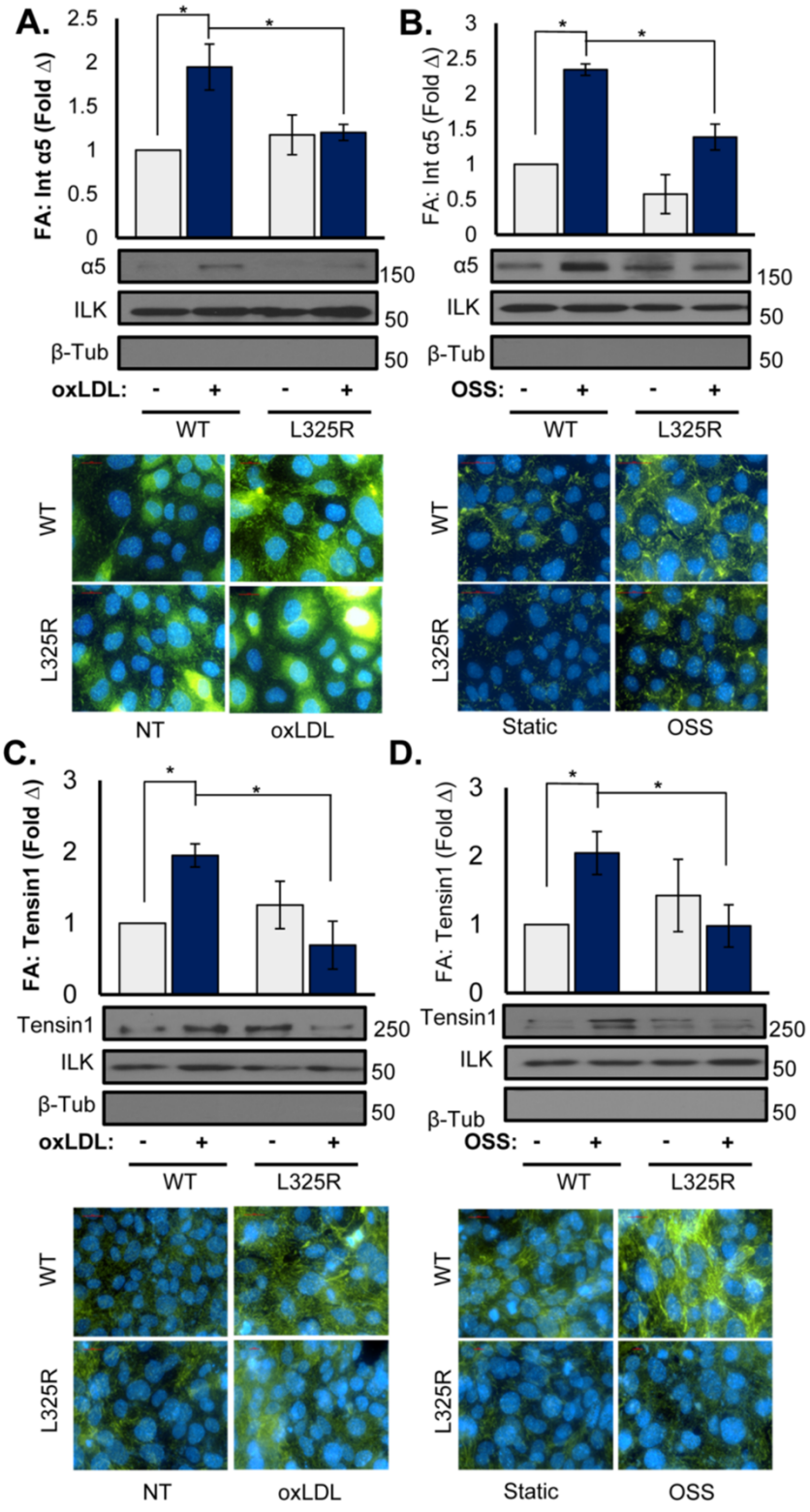

Figure 6. Talin1 L325R Endothelial Cells Show Reduction of α5 and Tenisn1 Localization in Integrin Adhesion in Response to Flow and OxLDL (oxidized low-density lipoprotein). A-B) Talin1 WT and Talin1 L325R cells were treated with oxLDL or exposed to OSS (oscillatory shear stress) for 18 hours and focal adhesions were extracted using hydrodynamic shock or stained for α5 integrins. Representative western blots (=4) and images are shown(n=3-4).C-D) A) Talin1 WT and Talin1 L325R cells were treated with oxLDL or exposed to OSS for 24 hours and focal adhesions were extracted or stained for tenisn1. Representative western blots images are shown(n=4-5). are shown(n=4). Values are means ±SE. *P<0.05 compared with 0 h time point. 2-way ANOVA with Bonferroni posttest was used for statistical analyses.

bioRxiv preprint doi: https://doi.org/10.1101/2020.02.14.949941; this version posted February 15, 2020. The copyright holder for this preprint (which was not certified by peer review) is the author/funder, who has granted bioRxiv a license to display the preprint in perpetuity. It is made available under aCC-BY-NC 4.0 International license.

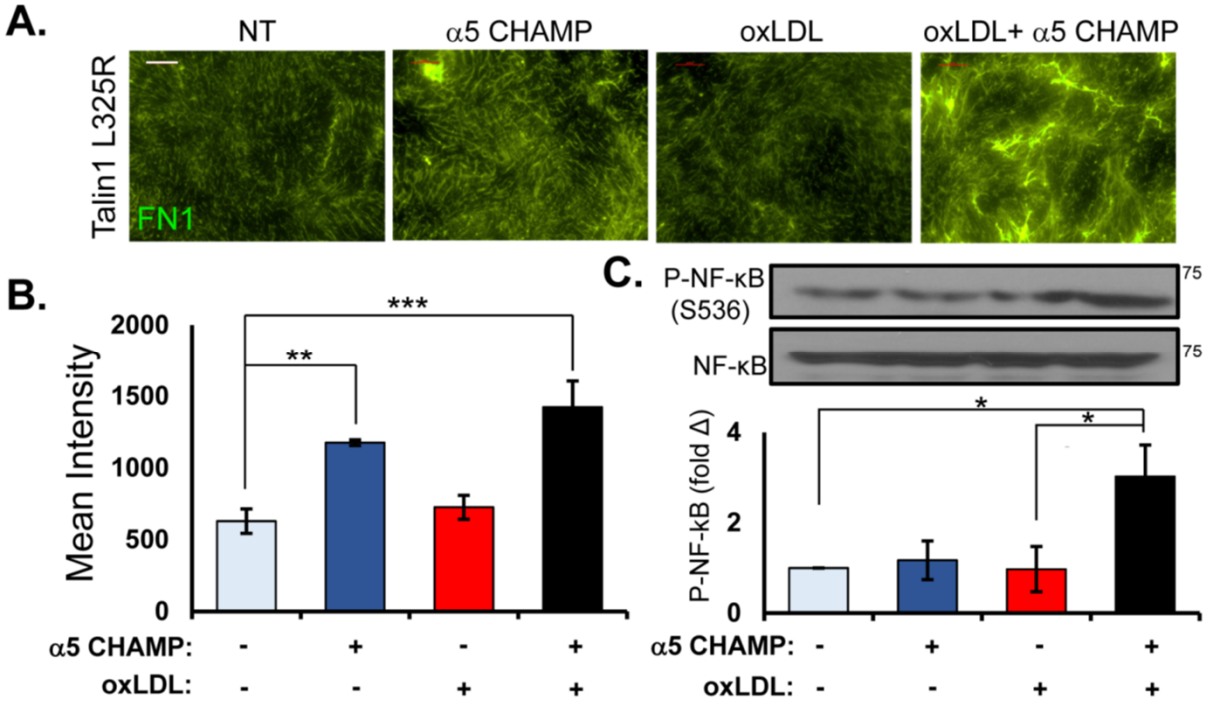

Figure 7. α5 Integrin Activation Requirement is Different for Matrix Remodeling Versus Inflammation. A)Talin1 L325R cells were plated on Matrigel for 4 hours, then treated with either oxLDL, α5 CHAMP, or both for 24 hours. Deoxycholate insoluble fractions were collected and immunocytochemistry was performed for fibronectin and quantified for mean fluorescent intensity. Representative images are shown(n=4-7). C. Talin1 L325R cells were plated on fibronectin and then treated with either oxLDL, α5 CHAMP, or both for 1 hours. Western blot was done for P-NF-κB (p65, Ser536). Representative blots are shown (n=4). Values are means ±SE. *P<0.05, **P<0.01 ***P<0.001 compared with 0 h time point. #p<0.05 compared with oxLDL group. two-way ANOVA with Bonferroni posttest was used for statistical analyses.

bioRxiv preprint doi: https://doi.org/10.1101/2020.02.14.949941; this version posted February 15, 2020. The copyright holder for this preprint (which was not certified by peer review) is the author/funder, who has granted bioRxiv a license to display the preprint in perpetuity. It is made available under aCC-BY-NC 4.0 International license.

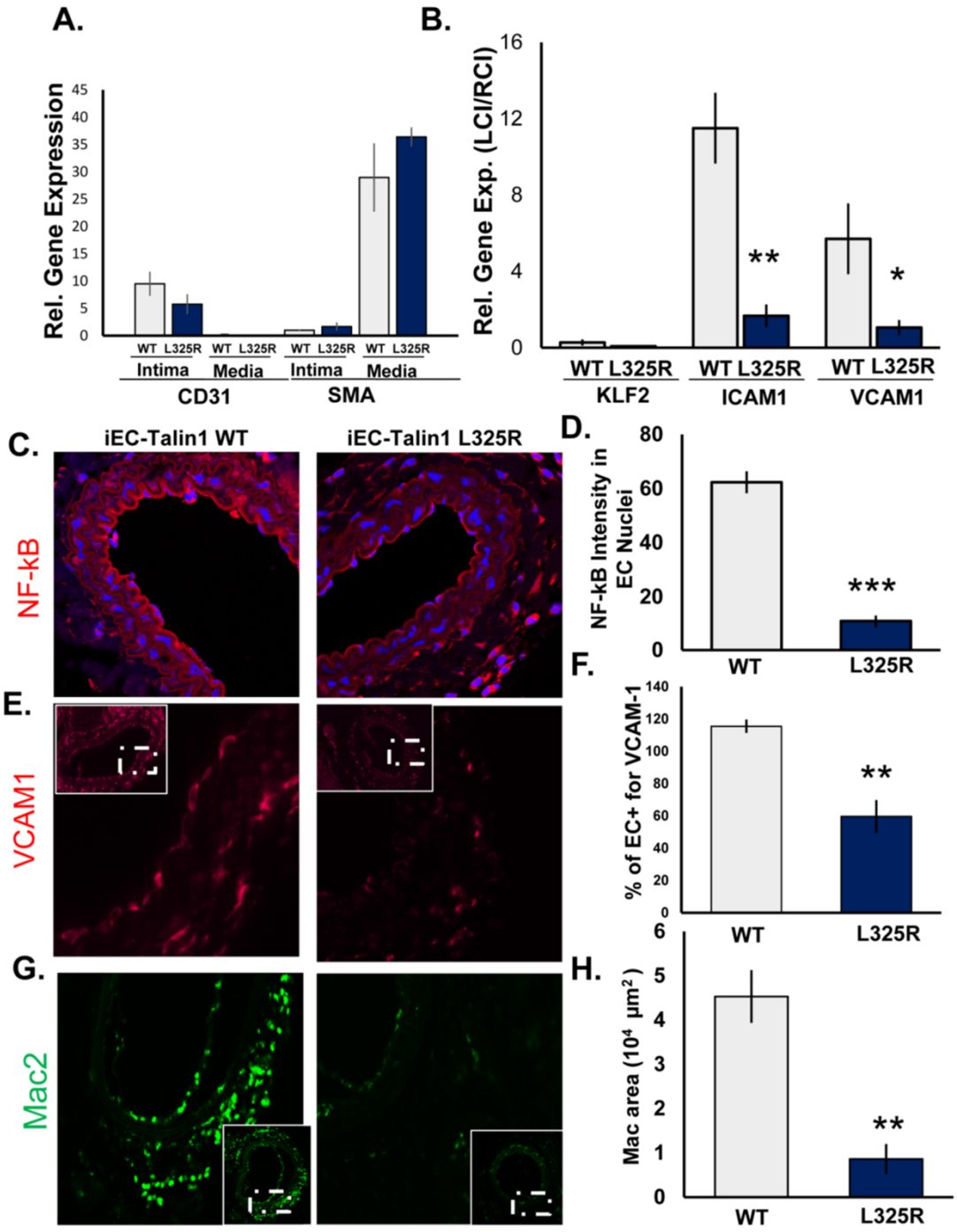

Figure 8. Mice Expressing Endothelial Talin1 325R Mutation Are Protected from Atherogenic Inflammation .A/B) iEC (inducible, endothelial cell-specific)-Talin1 WT (Talin1+/flox VE [vascular endothelial]-cadherin-CreERT2tg/?) and iEC Talin1 L325R -(Talin1flox/L325R VE-Cadherin- CreERT2tg) mice were treated with tamoxifen for 5 consecutive days. Four weeks later, mice underwent partial carotid ligation (PCL) of their left carotid artery for 48 hrs and the endothelial mRAN was isolated. Expression of CD31, SMA (A), Klf2, ICAM-1, and VCAM-1 (B) was determined by quantitative real-time PCR. n=5-6. **C-H)** iEC-Talin1 WT and iEC Talin1 L325R were undergone PCL for 7 day. Tissues were collected and immunohistochemistry for NF-κB (visualized by confocal microscopy), VCAM1, or Mac2 was conducted. N=5-6 for each group. F-H) After PCL for 7 days, immunohistochemistry was performed for MAC2(green) and SMA (red). Representative images are shown(n=5-6). Values are means ±SE. *P<0.05 and ***P<0.001 compared with 0 h time point. n.s. indicates not significant. Student t test was used for statistical analyses.

bioRxiv preprint doi: https://doi.org/10.1101/2020.02.14.949941; this version posted February 15, 2020. The copyright holder for this preprint (which was not certified by peer review) is the author/funder, who has granted bioRxiv a license to display the preprint in perpetuity. It is made available under aCC-BY-NC 4.0 International license.

Supplemental Table I

Antibodies

Target antigen	Vendor or Source	Catalog #	Working concentration
Phospho-NF-κB (Ser536, p65 subunit)	Cell Signaling Technology	#3033	1:1000 (WB)
NF-κB (p65 subunit)	Cell Signaling Technology	#4764	1:1000 (WB)
VCAM-1	Abcam	Ab134047	1:1000 (WB) 1:100 (IHC)
GAPDH	Cell Signaling Technology	#2118	1: 5000 (WB)
β-tubulin	Cell Signaling Technology	#2128	1:000 (WB)
ILK	Cell Signaling Technology	3856	1:000 (WB)
CD31	Santa Cruz	Sc-1506	4 μg/mL (IHC)
Mac2	Accurate Chemical	CL8942AP	0.1 μg/mL (IHC)
Smooth Muscle Actin	Sigma Aldrich	C6198	2.5 μg/ml (IHC)
Fibronectin	Sigma Aldrich	F3648	1:5000(WB)
α5 integrin	Abcam	ab150361	1:1000(WB)
β1 integrin	Santa Cruz	sc-374429	0.2ug/ml
Tensin 1	Sigma Aldrich	SAB4200283	1:1000 (WB)
P-p44/42 MAPK (ERK1/2) (Y204)	Cell Signaling Technology	#4370	1:1000 (WB)
ERK1/ERK2	Santa Cruz	sc-94	1:5000 (WB)
P-eNOS (Ser1177)	Cell Signaling Technology	#9571	1:500 (WB)
AKT 1/2	Santa Cruz	sc-1619	1:500 (WB)
P-AKT (Ser473)	Cell Signaling Technology	#4060	1:1000 (WB)
Paxillin	Cell Signaling Technology	#2542	1:1000 (WB)
Paxillin	Cell Signaling Technology	#2542	1:500 (ICC)
Vinculin	Sigma Aldrich	V4139	1:500 (ICC)

qRT-PCR Primers

Gene	Species	Forward	Reverse
β2- microglobulin	Mouse	TTCTGGTGCTTGTCTCACTGA	CAGTATGTTCGGCTTCCCATTC
Rpl13a	Mouse	GGGCAGGTTCTGGTATTGGAT	GGCTCGGAAATGGTAGGGG
KLF-2	Mouse	AGAATGCACCTGAGCCTGCTAG	AATTTCCCCGAAAGCCTGC
VCAM-1	Mouse	TCAAAGAAAGGGAGACTG	GCTGGAGAACTTCATTATC
ICAM-1	Mouse	CTGGCTGTCACAGAACAGGA	AAAGTAGGTGGGGAGGTGCT

bioRxiv preprint doi: https://doi.org/10.1101/2020.02.14.949941; this version posted February 15, 2020. The copyright holder for this preprint (which was not certified by peer review) is the author/funder, who has granted bioRxiv a license to display the preprint in perpetuity. It is made available under aCC-BY-NC 4.0 International license.

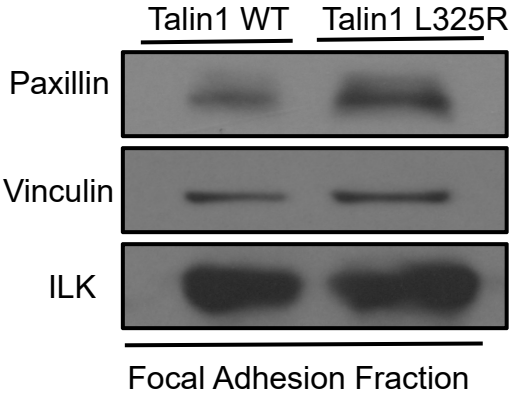

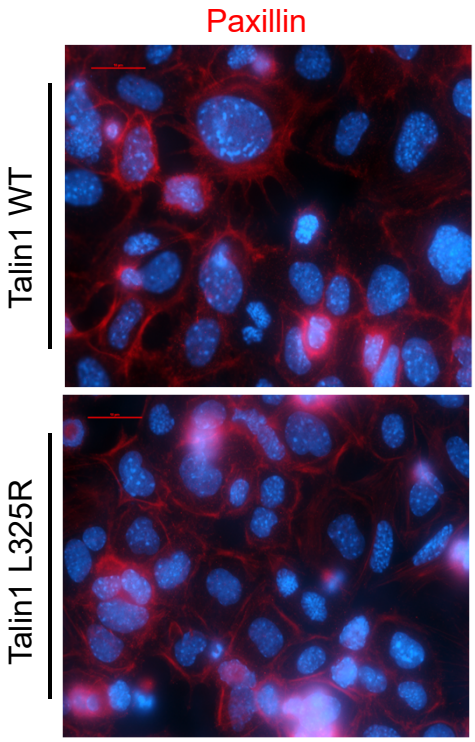

Supplemental Figure I. Talin1 L325R Mutation Does Not Alter Focal Adhesion Structure. Talin1 WT and Talin1 L325R cells were plated on fibronectin, then focal adhesions were extracted, or cells fixed for immunocytochemistry. Representative western blots and images are shown (n=3).

bioRxiv preprint doi: https://doi.org/10.1101/2020.02.14.949941; this version posted February 15, 2020. The copyright holder for this preprint (which was not certified by peer review) is the author/funder, who has granted bioRxiv a license to display the preprint in perpetuity. It is made available under aCC-BY-NC 4.0 International license.

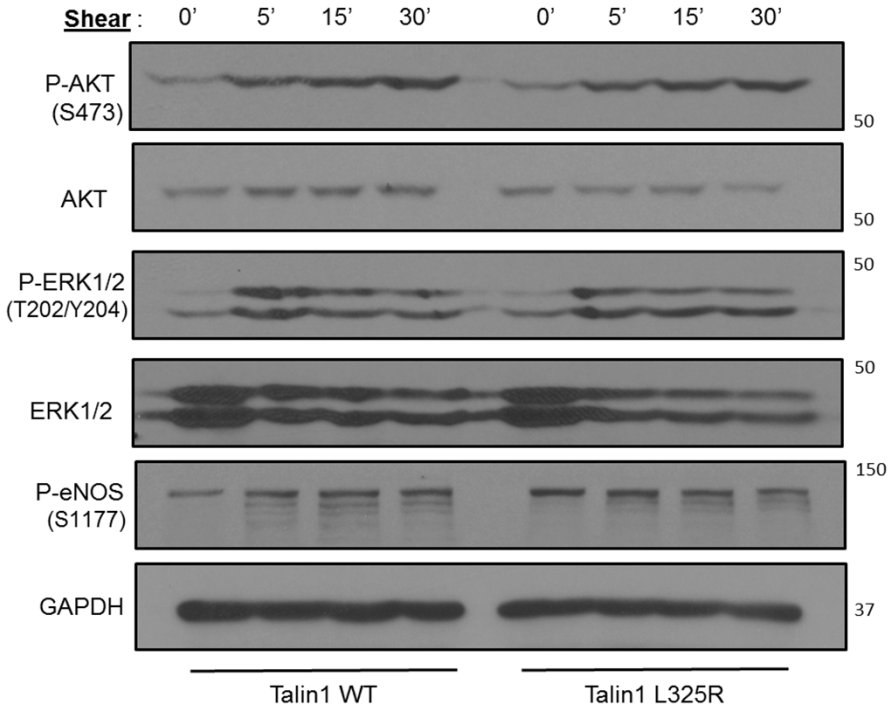

Supplemental Figure II. Talin1-dependent Integrin Activation isn't required for Shear Stress-Induced AKT/ERK/eNOS signaling. Talin1 WT and Talin1 L325R cells were exposed to shear stress for the indicated time points. Western blot was done using phospho-specific antibodies to measure activation of ERK, AKT, and eNOS. Representative western blots are shown(n=3).

bioRxiv preprint doi: https://doi.org/10.1101/2020.02.14.949941; this version posted February 15, 2020. The copyright holder for this preprint (which was not certified by peer review) is the author/funder, who has granted bioRxiv a license to display the preprint in perpetuity. It is made available under aCC-BY-NC 4.0 International license.

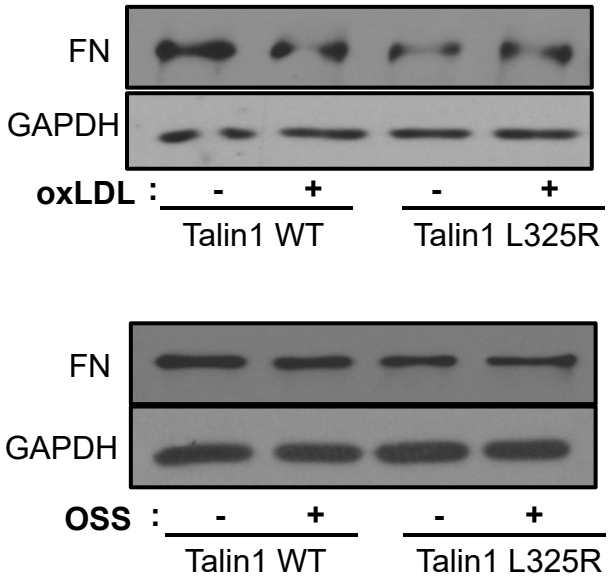

Supplemental Figure III. Intact Fibronectin Expression in Talin1 L325R Cells . Talin1 WT and Talin1 L325R cells were plated in Matrigel and then exposed to oxLDL or oscillatory shear stress for 24 hours.. Western blot was done using antibodies against fibronectin. n=3

bioRxiv preprint doi: https://doi.org/10.1101/2020.02.14.949941; this version posted February 15, 2020. The copyright holder for this preprint (which was not certified by peer review) is the author/funder, who has granted bioRxiv a license to display the preprint in perpetuity. It is made available under aCC-BY-NC 4.0 International license.

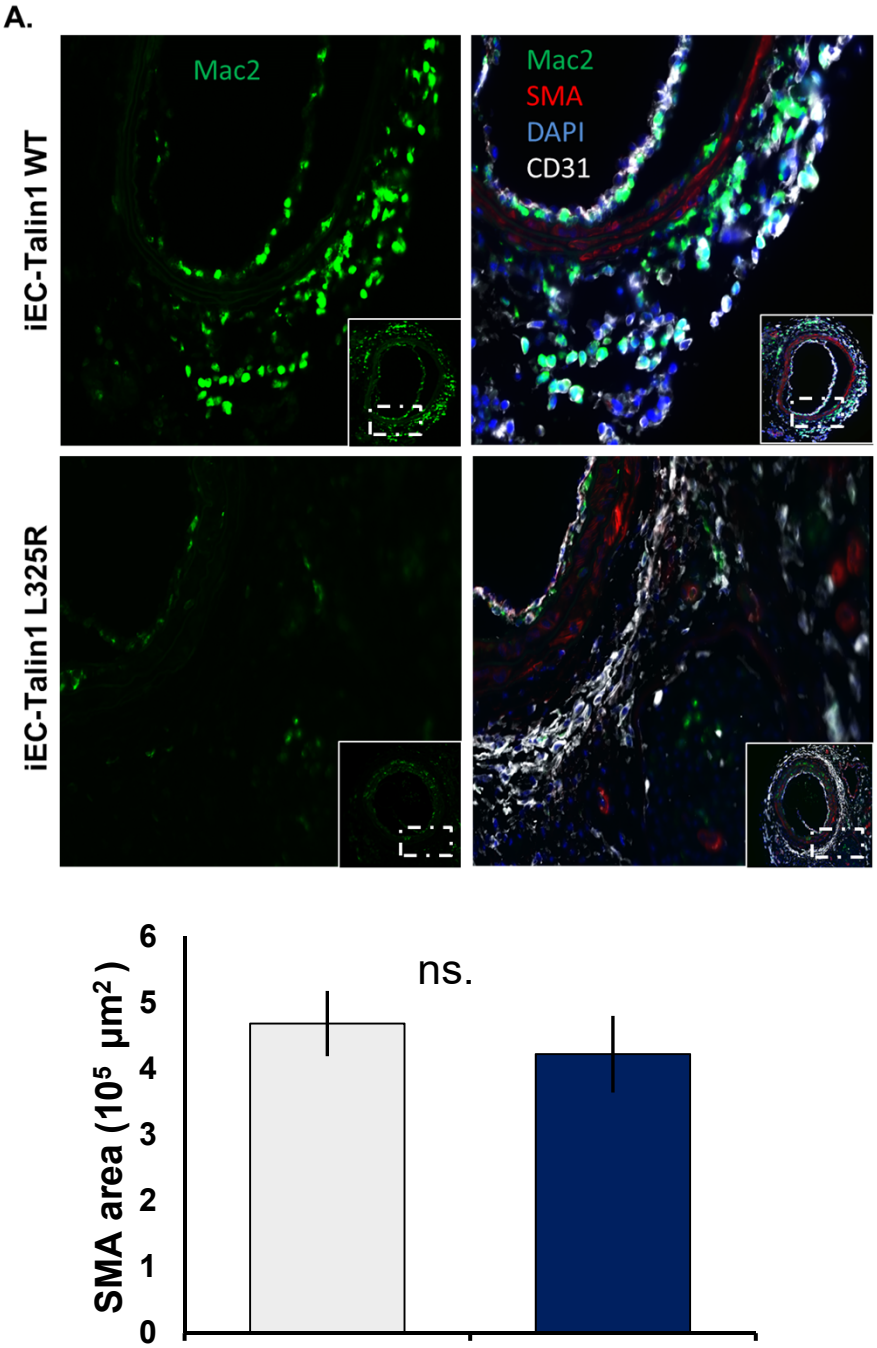

Supplemental Figure IV. Impaired Talin1-Dependent Integrin Activation Does Not Affect Endothelial Coverage or Smooth Muscle Cell Content. After PCL for 7 days, immunohistochemistry was performed for MAC2(green) and SMA (red). Representative images are shown(n=5-6). Values are means ±SE. n.s. indicates not significant. Student t test was used for statistical analysis.